Synthesis, Characterization, and Theoretical Investigation of a Transition State Analogue for Proton Transfer During C-H Activation by a Rhodium-Pincer Complex .

Joseph J. Gair,[b] Yehao Qiu,[b] Rahul L. Khade,[c] Natalie H. Chan,[a] Alexander S. Filatov,[b] Yong Zhang*[c] and Jared C. Lewis*[a].

[a]Department of Chemistry, Indiana University, Bloomington, Indiana 47405, United States

[b]Department of Chemistry, University of Chicago, Chicago, Illinois 60637, United States

[c]Department of Chemistry and Chemical Biology, Stevens Institute of Technology, Hoboken, New Jersey 07030, United States

ABSTRACT: A heterobimetallic rhodium-pincer complex bearing a phenylzinc ligand was synthesized and characterized by multinuclear NMR, COSY, NOESY, and X-ray crystallography. The crystal structure of this complex shows that it possesses a bridging Rh-Zn-C fragment with a geometry similar to the Rh-H-C fragment in a proposed transition state for metal-to-ligand proton transfer during redox-neutral C-H activation with dearomatized rhodium pincer complexes. Bonding analysis indicates that these fragments are isolobal, suggesting that the transition state analogue models not only the structure but also the bonding interactions that underlie metal-ligand cooperativity in the C-H activation transition state. The similarity of the transition state and its analogue prompted re-evaluation of the relevant rate equations to determine relative contributions of viable proton transfer pathways. Parallel analysis of the transition state and its isolobal analogue thus serves as a bridge between theory and experiment that is rarely available in studies of bonding in transition states.

Metal-ligand cooperativity can greatly expand the reactivity of transition metal complexes.[1,2] Complexes designed to harness bifunctional bond activation pathways—wherein both metal and ligand participate in bond formation and bond cleavage—have enabled the activation and catalytic functionalization of inert substrates.[3-9] Our group and others have been investigating the reactivity of 2,6-bis(di-*t*-butyl-phosphinomethyl)pyridine (PNP) complexes due to their ability to mediate challenging bond activations via metal-ligand cooperativity.[10-16] In particular, (PNP)Rh complexes are capable of cleaving aromatic C-H bonds at room temperature without the assistance of directing groups (Figure 1A).[15,17-20] This reactivity is uniquely enabled by deprotonation of the benzylic methylene in the PNP ligand (e.g. **1** to **2**), which leads to a dearomatized, strongly pi donating ligand. The increased electron density on rhodium from the dearomatized pi system promotes C-H cleavage via greater donation to the substrate C-H σ* orbital to generate Rh(III) hydride **3**.[21-23] After C-H oxidative addition, the deprotonated methylene acts as a base and reductant by accepting a proton to give Rh(I) complex **4**.[17] Without assistance from metal-ligand cooperativity, however, complex **1** is inert toward C-H activation.

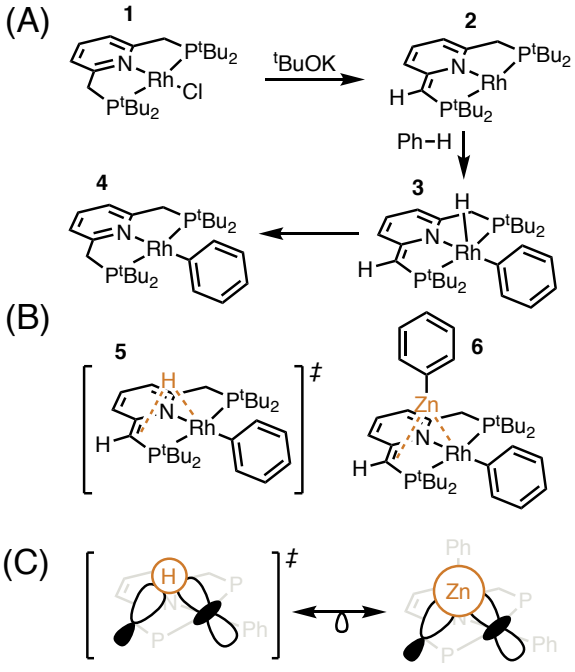

Figure 1. (A) Mechanism of C-H activation via metal-ligand cooperation; (B) Transition state **5** and transition state analogue **6**; (C) Representation of hypothesized isolobal relationship between bridging fragments in **5** and **6**.

The ability of metal-ligand cooperativity to enable otherwise inaccessible C-H bond activation by (PNP)Rh complexes has motivated detailed investigations into how metal and ligand act in concert to promote new reactivity in these systems. An essential aspect of this cooperative activation, the mechanism of metal-to-ligand proton transfer (tautomerization of **3** to **4**) , remains poorly understood. Perhaps the most direct pathway for tautomerization is through the proton-bridged transition state **5** (Figure 1B). The geometry of **5**, however, is qualitatively similar to the strained transition state that prevents β-hydride elimination in metallacylopentanes.[24-26] Indeed, a computational investigation of the corresponding iridium complexes evaluated the viability of a transition state analogous to **5** but found that the strained geometry of the proton-bridged metallabicycle resulted in a high barrier to direct proton transfer.[27,28]

Given the high energy of the proton-bridged transition state, the authors also examined pathways involving bridging water(s) and found that these resulted in a lower calculated barriers to proton transfer.[27,28] Intrigued by this result, we wondered whether these lower barriers would translate to increased relative rates for conversion of **3** to **4** when water concentration was considered (Figure S7). Analysis of the relevant rate equations involving 0-2 water molecules indicates that water-mediated pathways only become favorable when water concentration approaches 1 ppm. Below this water concentration, which can be readily achieved using molecular sieves,[29] direct proton transfer involving transition state **5** becomes favorable (Figure S8).

Given the relevance and unique geometry of transition state **5**, isolation of transition state analogue **6** (Figure 1B) during a study of direct arylation catalyzed by **1**[15] piqued our interest. We hypothesized that the same orbital interactions that mediate metal-to-ligand proton transfer in **5** might also be responsible for stabilizing the unusual geometry of **6** (Figure 1C). If the isolobal analogy held between these complexes, then **6** would serve as a model for bonding and metal-ligand cooperativity in transition state **5**.

Complex **6** was prepared by heating **4** with diphenylzinc at 70 °C for 18 hours (Figure 2A).[19,20] There are many examples of Rh-Zn[30-33] complexes, which have been reviewed[34,35] in the context of metal-metal bonding in metal-only Lewis acid/base pairs. There are notable instances of Rh-Zn complexes supported by (PNP) pincer ligands.[19,20,36] The structure of **6** in solution was determined by multinuclear NMR, COSY, and NOESY. The solid-state structure of **6** was determined by single crystal X-ray diffraction (Figure 2B). The contracted C1-C2 interatomic distance (C1-C2 1.44Å vs C3-C4 1.51Å) is consistent with partial double bond character and supports the assigned dearomatized structure.[37] The most notable structural feature of **6** is the zinc fragment which bridges between C1 and Rh.[34,35,38-41] The C1-Zn distance (2.20Å) is greater than the sum of the covalent radii (1.98Å)[42] and the geometry about C1 is distorted away from sp^3 and most closely resembles an sp^2 carbon with a lone pair localized in a p orbital donating to Zn (C2-C1-Zn 89°, P1-C1-Zn 87°, P1-C1-C2 114°). The long C1-Zn distance positions Zn in proximity to rhodium (Rh-Zn 2.52Å) and within the sum of Rh and Zn covalent radii (2.64Å).[42]

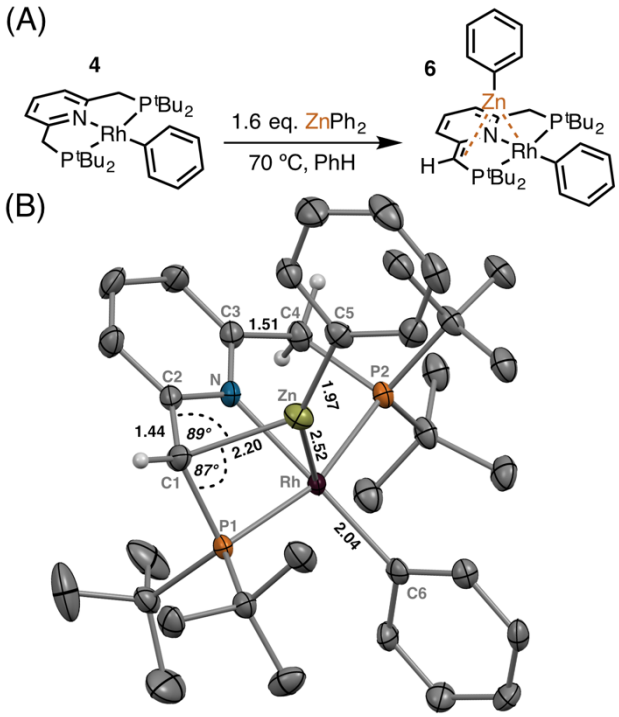

Figure 2. (A) Synthesis of complex **6** from complex **4** with $ZnPh_2$; (B) ORTEP of complex **6** with 50% thermal ellipsoids and non-essential hydrogens removed for clarity: selected bond distance (Å) and angles (deg) C1-C2 1.44, C3-C4 1.51, Rh-Zn 2.52, C1-Zn 2.20, Zn-C5 1.97, Rh-C6 2.04, C2-C1-Zn 89, P1-C1-Zn 87, P1-C1-C2 114, C1-Zn-Rh 79.

To compare bonding between the C_{benzyl}-Z-Rh fragments in compound **6** and transition state **5**, the structures of both compounds were optimized using density functional theory (Z = H or Zn in **5** and **6**, respectively). The calculated structure of **6** agreed well with the observed solid state geometry (Fig. 2b) (See table S1 for a comparison of geometric parameters and figure S3 for and image of overlaid structures). The structure of **5** was also similar to the previously calculated transition state of the iridium congener.[27] The calculated wave functions of these compounds were analyzed using the quantum theory of atoms in molecules (QTAIM), which holds that bonded atoms are linked by a bond path (a vector defined by maximal electron density, $\rho(\mathbf{r})$) and that on the bond path lies a bond critical point (BCP) at which the first derivative of $\rho(\mathbf{r})$ is zero.[43-45] Importantly, the topological features of $\rho(\mathbf{r})$ and the Laplacian of this value, $\nabla^2\rho(\mathbf{r})$, offer insight into the nature of bonding interactions.[44] As shown in Figure 3, bond paths and BCPs between C···Z and Rh···Z (Z = H and Zn) were successfully located, indicating that the Rh···H, Rh···Zn, C···H, and C···Zn interactions are bonding in nature. Based on their positive $\nabla^2\rho(\mathbf{r})$ values and negative total energy densities, H(**r**)'s, bonding between these atoms can be classified as electrostatic with partial covalence (Table 1). These data suggest that transition state analogue **6** bears qualitatively similar bonding features with **5**.

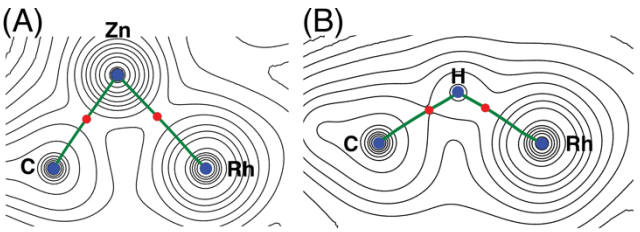

Figure 3. Contour line diagram of $\nabla^2\rho(\mathbf{r})$ for (A) complex **6** in the Rh-Zn-C plane and (B) transition state **5** in the Rh-H-C plane. Green lines connecting atoms in blue are bond paths and red circles are bond critical points.

Charge density may also be used to assess bonding strength in similar systems, with stronger bonds usually having larger $\rho(\mathbf{r})$ and shorter bond distance.[46] This allows for comparison of **5** to other complexes in which a hydrogen atom interacts with a transition metal, including metal hydrides and complexes that exhibit hydrogen bonding,[47] preagostic, or agostic interactions.[48] The $\rho(\mathbf{r})$ data in Table 1 show that the Rh···H interaction in **5** has greater charge density at the BCP than typical M···H interactions and is more similar to a metal hydride, consistent with relatively little M-H bond cleavage in the metal-to-ligand proton transfer transition state. The magnitude of the charge density at the BCP for the Rh···Zn interaction in **6** is less than that for the Rh···H interaction in **5**. Overall, however, the topology of the charge density at the BCPs between Rh-Z and C-Z indicates similar bonding in **5** and **6**.

Table 1. Selected Bond Critical Point Properties.[a]

Complex	Bond	R (Å)	ρ(r) (au)	∇²ρ(r) (au)	H(r)(au)
5	Rh···H	1.742	0.10277	0.03316	-0.0489
6	Rh···Zn	2.582	0.04897	0.06868	-0.0172
7[b]	Preagostic	2.3~3.0	0.01~0.03	0.03~0.07	-0.001
	C-H...M				~0.001
8[c]	Agostic	1.8~2.3	0.04~0.05	0.15~0.25	n/a
	C-H...M				
9[d]	M-H	1.4~1.9	0.13~0.16	0.01~0.2	n/a

[a]See SI for full list of properties. [b]Data are for M…H preagostic and hydrogen bonding (HB) interactions from Ref.[49] [c]Geometric data and AIM results are from Ref.[50] and Ref.[51] respectively. [d]Geometric and QTAIM data for metal hydrides are from Ref[52] and Ref [32,53 54] respectively.

Given the similar geometry and bonding about the bridging C_{benzyl}-Z-Rh fragments in **5** and **6**, we sought to assess whether the orbital interactions that stabilize the unusual geometry of the transition state analogue (**6**) are similar to those that promote metal-ligand cooperativity in **5**. Whereas transition state analogues mimic structure, they need not reflect the bonding of the corresponding transition state.[55] Toward this end, the isolobal analogy describes bonding similarities between structurally diverse molecular fragments.[56] Specifically, Hoffmann defined two fragments as being isolobal "if the number, symmetry properties, approximate energy, and shape of the frontier orbitals and the number of electrons in them are similar-not identical, but similar".[56] Thus, we wanted to establish whether **5** and **6** are isolobal, as introduced qualitatively in Fig. 1C, and thus whether **6** serves as a model for not only the structure but also bonding in **5**. The relevant bonding interactions were assessed using second order natural bond orbital (NBO) perturbation theory to identify stabilizing donor-acceptor pairs of NBOs (Figure 4).[57]

The bridging fragments in both **5** and **6** are stabilized by two major donor-acceptor interactions. In transition state **5** a rhodium d orbital donates to the 1s orbital on the bridging hydrogen: 4d(Rh) → 1s(H) (Figure 5B → C). The second stabilizing pair in transition state **5** involves donation from a π(C-C) bonding NBO on the dearomatized ligand to the LUMO of the bridging proton: π(C-C) → 1s(H) (Figure 5D → C). These donor-acceptor interactions to the bridging hydrogen in transition state **5** are overlaid in Figure 5E. In complex **6**, a rhodium d orbital donates to the empty nonbonding orbital on the bridging Zn: 4d(Rh) → 4s(Zn) (Figure 5G → H). The second stabilizing pair in complex **6** involves donation from a lone pair localized in a primarily p orbital on the deprotonated ligand to the LUMO of the bridging Zn: 2p(C) → 4s(Zn) (Figure 5I → H). These donor-acceptor interactions to the bridging Zn fragment in transition state analog **6** are overlaid in Figure 5J.

As hypothesized above, this analysis is consistent with an isolobal relationship between the NBOs localized on the bridging fragments in **5** and **6** that contribute to the largest stabilizing interactions on those fragments. Specifically, in both interactions (and in both structures) the acceptor is an s type NBO localized on the bridging atom; namely, a low occupancy 1s type NBO on H^+ in **5** and a low occupancy 4s type NBO on $PhZn^+$ in **6**. The four NBOs which donate into bridging s-type NBOs, on the other hand, are somewhat varied. It is worth noting, however, that despite the variation in their composition, all four donor NBOs interact with the bridging acceptors with the same (σ) symmetry.

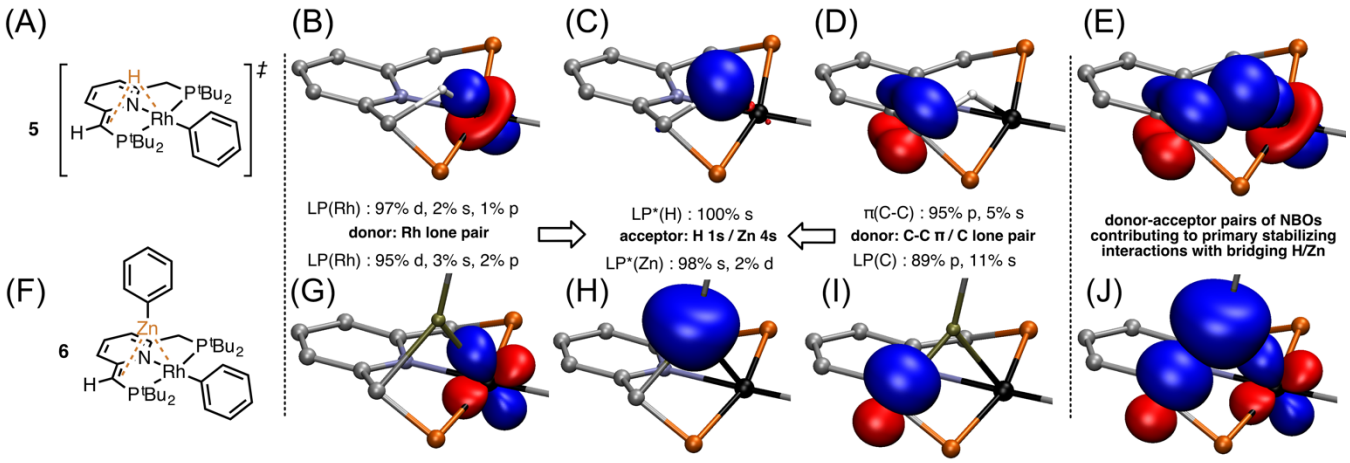

Figure 4. Summary of stabilizing donor acceptor pairs from second order NBO perturbation theory (A) representation of transition state **5** (B) Donor NBO in **5**, 4d(Rh) (C) Acceptor NBO in **5**, 1s(H) (D) Donor NBO in **5**, π(C-C) (E) Overlaid NBO donors and acceptor that contribute to stabilizing the bridging proton in **5** (F) representation of transition state analog **6** (G) Donor NBO in **6**, 4d(Rh) (H) Acceptor NBO in **6**, 4s(Zn) (I) Donor NBO **6**, 2p(C) (J) Overlaid NBO donors and acceptor that contribute to stabilizing the bridging Zn in **6**.

The structures of transition states cannot be experimentally characterized for any but the simplest reactions.[58,59] Transition state analogues, however, can be experimentally characterized to provide insight into the nature of transition state structures[60-62] as evidenced by the exquisite binding affinities of transition state analogues toward target enzymes.[63] As previously noted, however, transition state analogues typically do not serve as models for bonding in the transition states that they mimic. Because transition state structures are experimentally elusive, our understanding of bonding interactions in transition states is therefore limited to analysis of calculated structures that possess intuitively reasonable geometries. Differing opinions of what constitutes "reasonable" and the accuracy of computed energies are critical considerations in this approach to understanding transitions states.

In this report, observation of a transition state analogue that mimics the strained geometry of transition state **5** led us to re-evaluate the relevant rate equations for various pathways to proton transfer (supporting information Figure S7). This analysis suggests that multiple pathways (water-mediated and direct proton transfer) are relevant to cooperative C-H activation and that, despite its strained geometry, transition state **5** is the favored pathway for metal-to-ligand proton transfer under rigorously anhydrous reaction conditions (<1 ppm water). A bonding analysis of the putative transition state and the corresponding transition state analogue revealed that the same type of orbital interactions that stabilize the unusual geometry of **6** also support metal-to-ligand proton transfer during C-H activation involving **5**. More generally, experimental observation of the geometry of an isolobal transition state analogue, in parallel with computational analysis of bonding in the transition state and the analogue, provides a means to achieve the synergistic feedback between observation and computation during mechanistic studies that can both motivate and validate our understanding of the unique geometries and bonding interactions present in transition states.

ASSOCIATED CONTENT

Supporting Information

The Supporting Information is available free of charge on the ACS Publications website.

Synthetic and Computational Procedures (PDF)
Coordinates of Calculated Structures (XYZ)

CCDC 1579252 and 1843053-1843054 contain the supplementary crystallographic data for this paper. These data can be obtained free of charge via www.ccdc.cam.ac.uk/data_request/cif, or by emailing data_request@ccdc.cam.ac.uk, or by contacting The Cambridge Crystallographic Data Centre, 12 Union Road, Cambridge CB2 1EZ, UK; fax: +44 1223 336033.

AUTHOR INFORMATION

Corresponding Author

* Email for JCL: jcl3@iu.edu

ORCID

Jared C. Lewis: 0000-0003-2800-8330
Joseph J. Gair: 0000-0002-2139-4702
Yong Zhang: 0000-0001-7207-6416

Notes

The authors declare no competing financial interest..

ACKNOWLEDGMENT

We would like to thank Brandon E. Haines and Jonathan H. Skone for helpful discussions.

This work was supported by the NSF under the CCI Center for Selective C-H Functionalization (CCHF, CHE-1205646) and by a US NSF grant CHE-1300912 to YZ. JJG was supported by an NSF predoctoral fellowship (DGE-1144082). This work was completed in part with resources provided by the University of Chicago Research Computing Center. Use of the Advanced Photon

Source, an Office of Science User Facility operated for the U.S. Department of Energy (DOE) Office of Science by Argonne National Laboratory, was supported by U.S. DOE under contract No. DE-AC02-06miltCH11357. ChemMatCARS Sector 15 is principally supported by the Divisions of Chemistry (CHE) and Materials Research (DMR), National Science Foundation, under grant number NSF/CHE-1346572.

REFERENCES

(1) Khusnutdinova, J. R.; Milstein, D. Metal-Ligand Cooperation. *Angew. Chem. Int. Ed.* **2015**, *54*, 12236–12273.

(2) Gunanathan, C.; Milstein, D. Metal–Ligand Cooperation by Aromatization–Dearomatization: a New Paradigm in Bond Activation and "Green" Catalysis. *Acc. Chem. Res.* **2011**, *44*, 588–602.

(3) van der Vlugt, J. I.; Reek, J. N. H. Neutral Tridentate PNP Ligands and Their Hybrid Analogues: Versatile Non-Innocent Scaffolds for Homogeneous Catalysis. *Angew. Chem. Int. Ed. Engl.* **2009**, *48*, 8832–8846.

(4) Milstein, D. Metal-Ligand Cooperation by Aromatization-Dearomatization as a Tool in Single Bond Activation. *Philos Trans A Math Phys Eng Sci* **2015**, *373*.

(5) Gunanathan, C.; Milstein, D. Bond Activation by Metal-Ligand Cooperation: Design of "Green" Catalytic Reactions Based on Aromatization-Dearomatization of Pincer Complexes. In *Bifunctional Molecular Catalysis*; Ikariya, T.; Shibasaki, M., Eds.; Topics in Organometallic Chemistry; Springer Berlin Heidelberg: Berlin, Heidelberg, 2011; Vol. 37, pp. 55–84.

(6) Annibale, V. T.; Song, D. Multidentate Actor Ligands as Versatile Platforms for Small Molecule Activation and Catalysis. *RSC Adv.* **2013**, *3*, 11432–18.

(7) van der Vlugt, J. I. Cooperative Catalysis with First-Row Late Transition Metals. *Eur. J. Inorg. Chem.* **2011**, *2012*, 363–375.

(8) Grützmacher, H. Cooperating Ligands in Catalysis. *Angew. Chem. Int. Ed. Engl.* **2008**, *47*, 1814–1818.

(9) Benito-Garagorri, D.; Kirchner, K. Modularly Designed Transition Metal PNP and PCP Pincer Complexes Based on Aminophosphines: Synthesis and Catalytic Applications. *Acc. Chem. Res.* **2008**, *41*, 201–213.

(10) Ben Ari, E.; Leitus, G.; Shimon, L. J. W.; Milstein, D. Metal–Ligand Cooperation in C–H and H 2Activation by an Electron-Rich PNP Ir(I) System: Facile Ligand Dearomatization–Aromatization as Key Steps. *J. Am. Chem. Soc.* **2006**, *128*, 15390–15391.

(11) Bernskoetter, W. H.; Schauer, C. K.; Goldberg, K. I.; Brookhart, M. Characterization of a Rhodium(I) -Methane Complex in Solution. *Science* **2009**, *326*, 553–556.

(12) Semproni, S. P.; Hojilla Atienza, C. C.; Chirik, P. J. Oxidative Addition and C–H Activation Chemistry with a PNP Pincer-Ligated Cobalt Complex. *Chem. Sci.* **2014**, *5*, 1956–5.

(13) Kuriyama, S.; Arashiba, K.; Nakajima, K.; Tanaka, H.; Yoshizawa, K.; Nishibayashi, Y. Nitrogen Fixation Catalyzed by Ferrocene-Substituted Dinitrogen-Bridged Dimolybdenum–Dinitrogen Complexes: Unique Behavior of Ferrocene Moiety as Redox Active Site. *Chem. Sci.* **2015**, *00*, 1–12.

(14) Huff, C. A.; Kampf, J. W.; Sanford, M. S. Role of a Noninnocent Pincer Ligand in the Activation of CO 2at (PNN)Ru(H)(CO). **2012**, *31*, 4643–4645.

(15) Gair, J. J.; Qiu, Y.; Chan, N. H.; Filatov, A. S.; Lewis, J. C. Rhodium Complexes of 2,6-Bis(Dialkylphosphinomethyl)Pyridines: Improved C–H Activation, Expanded Reaction Scope, and Catalytic Direct Arylation. **2017**, *36*, 4699–4706.

(16) Bailey, W. D.; Kaminsky, W.; Kemp, R. A.; Goldberg, K. I. Synthesis and Characterization of Anionic, Neutral, and Cationic PNP Pincer Pd IIand Pt IIHydrides. **2014**, *33*, 2503–2509.

(17) Schwartsburd, L.; Iron, M. A.; Konstantinovski, L.; Ben Ari, E.; Milstein, D. A Dearomatized Anionic PNP Pincer Rhodium Complex: C–H and H–H Bond Activation by Metal–Ligand Cooperation and Inhibition by Dinitrogen. **2011**, *30*, 2721–2729.

(18) Anaby, A.; Feller, M.; Ben-David, Y.; Leitus, G.; Diskin-Posner, Y.; Shimon, L. J. W.; Milstein, D. Bottom-Up Construction of a CO2-Based Cycle for the Photocarbonylation of Benzene, Promoted by a Rhodium(I) Pincer Complex. *J. Am. Chem. Soc.* **2016**, *138*, 9941–9950.

(19) Kloek, S. M.; Heinekey, D. M.; Goldberg, K. I. C-H Bond Activation by Rhodium(I) Hydroxide and Phenoxide Complexes. *Angew. Chem. Int. Ed. Engl.* **2007**, *46*, 4736–4738.

(20) Hanson, S. K.; Heinekey, D. M.; Goldberg, K. I. C–H Bond Activation by Rhodium(I) Phenoxide and Acetate Complexes: Mechanism of H–D Exchange Between Arenes and Water. **2008**, *27*, 1454–1463.

(21) Ess, D. H.; Goddard, W. A., III; Periana, R. A. Electrophilic, Ambiphilic, and Nucleophilic C–H Bond Activation: Understanding the Electronic Continuum of C–H Bond Activation Through Transition-State and Reaction Pathway Interaction Energy Decompositions. **2010**, *29*, 6459–6472.

(22) Krogh-Jespersen, K.; Czerw, M.; Zhu, K.; Singh, B.; Kanzelberger, M.; Darji, N.; Achord, P. D.; Renkema, K. B.; Goldman, A. S. Combined Computational and Experimental Study of Substituent Effects on the Thermodynamics of H 2, CO, Arene, and Alkane Addition to Iridium. *J. Am. Chem. Soc.* **2002**, *124*, 10797–10809.

(23) Wang, D. Y.; Choliy, Y.; Haibach, M. C.; Hartwig, J. F.; Krogh-Jespersen, K.; Goldman, A. S. Assessment of the Electronic Factors Determining the Thermodynamics of "Oxidative Addition" of C-H and N-H Bonds to Ir(I) Complexes. *J. Am. Chem. Soc.* **2016**, *138*, 149–163.

(24) McDermott, J. X.; White, J. F.; Whitesides, G. M. Preparation and Thermal Decomposition of Platinum(II) Metallocycles. *J. Am. Chem. Soc.* **1973**, *95*, 4451–4452.

(25) McDermott, J. X.; White, J. F.; Whitesides, G. M. Thermal Decomposition of Bis(Phosphine)Platinum(II) Metallocycles. *J. Am. Chem. Soc.* **1976**, *98*, 6521–6528.

(26) Miller, T. M.; Whitesides, G. M. Mechanism of Thermal Decomposition of Bis(Tricyclopentylphosphine)Platinacyclopentane(II): Intramolecular .Beta.-Hydride Elimination From the Platinacyclopentane Ring Is Slow Relative to an Intermolecular Chain Reaction Involving Hydridoplatinum Intermediates. **1986**, *5*, 1473–1480.

(27) Iron, M. A.; Ben Ari, E.; Cohen, R.; Milstein, D. Metal–Ligand Cooperation in the Trans Addition of Dihydrogen to a Pincer Ir(I) Complex: a DFT Study. *Dalton Trans.* **2009**, 9433–9437.

(28) Li, H.; Hall, M. B. Computational Mechanistic Studies on Reactions of Transition Metal Complexes with Noninnocent Pincer Ligands: Aromatization–Dearomatization or Not. *ACS Catal.* **2015**, *5*, 1895–1913.

(29) Burfield, D. R.; Lee, K.-H.; Smithers, R. H. Desiccant Efficiency in Solvent Drying. a Reappraisal by Application of a Novel Method for Solvent Water Assay. *J. Org. Chem.* **1977**, *42*, 3060–3065.

(30) Cadenbach, T.; Bollermann, T.; Gemel, C.; Tombul, M.; Fernandez, I.; Hopffgarten, M. V.; Frenking, G.; Fischer, R. A. Molecular Alloys, Linking Organometallics with Intermetallic Hume–Rothery Phases: the Highly Coordinated Transition Metal Compounds [M(ZnR) N] (N≥ 8) Containing Organo–Zinc Ligands. *J. Am. Chem. Soc.* **2009**, *131*, 16063–16077.

(31) Molon, M.; Cadenbach, T.; Bollermann, T.; Gemel, C.; Fischer, R. A. One Electron Organozinc Ligands in Metal Rich Molecules by Ga/Zn Exchange: From Cp*Rh(GaCp*)2 to Cp*Rh(ZnR)4 Units. *Chem. Commun.* **2010**, *46*, 5677–3.

(32) Ekkert, O.; White, A. J. P.; Toms, H.; Crimmin, M. R. Addition of Aluminium, Zinc and Magnesium Hydrides to Rhodium(Iii). *Chem. Sci.* **2015**, *6*, 5617–5622.

(33) Ekkert, O.; White, A. J. P.; Crimmin, M. R. Trajectory of Approach of a Zinc-Hydrogen Bond to Transition Metals. *Angew. Chem.* **2016**, *128*, 16265–16268.
(34) Bollermann, T.; Gemel, C.; Fischer, R. A. Organozinc Ligands in Transition Metal Chemistry. *Coordination Chemistry Reviews* **2011**, *256*, 537–555.
(35) Bauer, J.; Braunschweig, H.; Dewhurst, R. D. Metal-Only Lewis Pairs with Transition Metal Lewis Bases. *Chem. Rev.* **2012**, *112*, 4329–4346.
(36) Pell, C. J.; Shih, W.-C.; Gatard, S.; Ozerov, O. V. Formation of (PNP)Rh Complexes Containing Covalent Rhodium-Zinc Bonds in Studies of Potential Rh-Catalysed Negishi Coupling. *Chem. Commun.* **2017**, *53*, 6456–6459.
(37) Schwartsburd, L.; Iron, M. A.; Konstantinovski, L.; Diskin-Posner, Y.; Leitus, G.; Shimon, L. J. W.; Milstein, D. Synthesis and Reactivity of an Iridium(I) Acetonyl PNP Complex. Experimental and Computational Study of Metal–Ligand Cooperation in H–H and C–H Bond Activation via Reversible Ligand Dearomatization. **2010**, *29*, 3817–3827.
(38) Oeschger, R. J.; Chen, P. A Heterobimetallic Pd–Zn Complex: Study of a D 8–D 10Bond in Solid State, in Solution, and in Silico. **2017**, *36*, 1465–1468.
(39) Oeschger, R. J.; Chen, P. Structure and Gas-Phase Thermochemistry of a Pd/Cu Complex: Studies on a Model for Transmetalation Transition States. *J. Am. Chem. Soc.* **2017**, *139*, 1069–1072.
(40) Paenurk, E.; Gershoni-Poranne, R.; Chen, P. Trends in Metallophilic Bonding in Pd–Zn and Pd–Cu Complexes. **2017**, *36*, 4854–4863.
(41) Baya, M.; Belío, Ú.; Fernandez, I.; Fuertes, S.; Martín, A. Unusual Metal-Metal Bonding in a Dinuclear Pt-Au Complex: Snapshot of a Transmetalation Process. *Angew. Chem.* **2016**, *128*, 7092–7096.
(42) Cordero, B.; Gómez, V.; Platero-Prats, A. E.; Revés, M.; Echeverría, J.; Cremades, E.; Barragán, F.; Alvarez, S. Covalent Radii Revisited. *Dalton Trans.* **2008**, *40*, 2832–2837.
(43) Bader, R. F. W. Molecular Fragments or Chemical Bonds. *Acc. Chem. Res.* **1974**, *8*, 34–40.
(44) Bader, R. F. W. A Quantum Theory of Molecular Structure and Its Applications. *Chem. Rev.* **1991**, *91*, 893–928.
(45) Bader, R. F. W. Bond Paths Are Not Chemical Bonds. *J. Phys. Chem. A* **2009**, *113*, 10391–10396.
(46) Cheng, F.; Sun, H.; Zhang, Y.; Mukkamala, D.; Oldfield, E. A Solid State 13C NMR, Crystallographic, and Quantum Chemical Investigation of Chemical Shifts and Hydrogen Bonding in Histidine Dipeptides. *J. Am. Chem. Soc.* **2005**, *127*, 12544–12554.
(47) Brammer, L. Metals and Hydrogen Bonds. *Dalton Trans.* **2003**, 3145–13.
(48) Brookhart, M.; Green, M. L. H.; Parkin, G. Agostic Interactions in Transition Metal Compounds. *Proceedings of the National Academy of Sciences* **2007**, *104*, 6908–6914.
(49) Zhang, Y.; Lewis, J. C.; Bergman, R. G.; Ellman, J. A.; Oldfield, E. NMR Shifts, Orbitals, and M···H–X Bonding in D 8Square Planar Metal Complexes. **2006**, *25*, 3515–3519.
(50) Yao, W.; Eisenstein, O.; Crabtree, R. H. Interactions Between C-H and N-H Bonds and D8 Square Planar Metal Complexes: Hydrogen Bonded or Agostic? *Inorganica Chimica Acta* **1997**, *254*, 105–111.
(51) Popelier, P. L. A.; Logothetis, G. Characterization of an Agostic Bond on the Basis of the Electron Density. *Journal of Organometallic Chemistry* **1998**, *555*, 101–111.
(52) Allen, F. H.; Bruno, I. J. Bond Lengths in Organic and Metal-Organic Compounds Revisited: X—H Bond Lengths From Neutron Diffraction Data. *Acta Cryst Sect A Found Cryst* **2010**, *66*, 380–386.
(53) Papp, T.; Kollar, L.; Kegl, T. Estimation of Bite Angle Effect on the Electronic Structure of Cobalt-Phosphine Complexes: a QTAIM Study. *Journal of Quantum Chemistry* **2014**, *2014*, 1–5.
(54) Hamdaoui, M.; Ney, M.; Sarda, V.; Karmazin, L.; Bailly, C.; Sieffert, N.; Dohm, S.; Hansen, A.; Grimme, S.; Djukic, J.-P. Evidence of a Donor–Acceptor (Ir–H)→SiR 3Interaction in a Trapped Ir(III) Silane Catalytic Intermediate. **2016**, *35*, 2207–2223.
(55) Powers, D. C.; Ritter, T. A Transition State Analogue for the Oxidation of Binuclear Palladium(II) to Binuclear Palladium(III) Complexes. **2013**, *32*, 2042–2045.
(56) Hoffmann, R. Building Bridges Between Inorganic and Organic Chemistry(Nobel Lecture). *Angew. Chem. Int. Ed. Engl.* **1982**, *21*, 711–724.
(57) Weinhold, F.; Landis, C. R. *Valency and Bonding: a Natural Bond Orbital Donor-Acceptor Perspective*; 2005.
(58) Wynne Jones, W. F. K.; Eyring, H. The Absolute Rate of Reactions in Condensed Phases. *J. Chem. Phys.* **1935**, *3*, 492–502.
(59) Polanyi, J. C.; Zewail, A. H. Direct Observation of the Transition State. *Acc. Chem. Res.* **2002**, *28*, 119–132.
(60) Wolfenden, R. Analog Approaches to the Structure of the Transition State in Enzyme Reactions. *Acc. Chem. Res.* **1972**, *5*, 10–18.
(61) Schramm, V. L. Enzymatic Transition State Theory and Transition State Analogue Design. *Journal of Biological Chemistry* **2007**, *282*, 28297–28300.
(62) Amyes, T. L.; Richard, J. P. Specificity in Transition State Binding: the Pauling Model Revisited. *Biochemistry* **2013**, *52*, 2021–2035.
(63) Schramm, V. L. Enzymatic Transition States, Transition-State Analogs, Dynamics, Thermodynamics, and Lifetimes. *Annu. Rev. Biochem.* **2011**, *80*, 703–732.

TOC Graphic: